Development of Advanced Nickelate-based Oxygen Electrodes for Solid Oxide Cells

M.A. Laguna-Bercero[a], A. Orera[a], M. Morales-Zapata[a,b], A. Larrea[a]

[a] Instituto de Ciencia de Materiales de Aragón, CSIC – U. Zaragoza, c/ María de Luna 3, E-50.018 Zaragoza, Spain

[b] Universidad Tecnológica de Panamá, av/ Ricardo J. Alfaro, Campus Víctor Levi Sasso, 0819-07289, Panama

The present work deals with the development of lanthanide nickelate based oxygen electrodes ($Ln_2NiO_{4+\delta}$, with Ln = Nd, La or Pr) as the oxygen electrode for solid oxide cells (SOCs) operating in both solid oxide fuel cell (SOFC) and solid oxide electrolysis (SOEC) modes. These compounds have been widely investigated as they present high oxygen diffusion properties, making them attractive as SOFC oxygen electrodes. However, the main drawback of these nickelate phases is their reactivity with standard YSZ (yttria stabilized zirconia) or CGO (cerium gadolinium oxide) electrolytes, as typical sintering temperatures are usually higher than 1000 ºC in order to get strong adhesion at the electrode/electrolyte interface. Two strategies will be employed to avoid the undesired reactivity: the direct formation of the nickelate phase into YSZ scaffolds by infiltration and the development of an active barrier layer.

Introduction

One of the important aspects to achieving long lifetime SOFCs and SOECs is to enhance the durability and performance of the oxygen electrode, as it typically degrades over time under the operating conditions. In addition, it is necessary to improve the phase stability at the electrode/electrolyte interface under high oxygen partial pressures (pO_2) in SOEC operation mode, and especially above ~ 750°C (1). As reported by several authors, this overpressure can lead to electronic reduction of the YSZ (2, 3). Virkar explained that this oxygen partial pressure increase phase occurs along the oxygen electrode/electrolyte interface. Severe cell degradation can be produced in form of voids, cracks and/or delamination of the oxygen electrode (4, 5, 6). In SOEC operation, this problem is still one of the major concerns and has been under investigation for the last decade. Recently, it has been shown that reversible operation either avoids the formation or, if previously formed, the growing of oxygen bubbles avoids its growing (7). The mechanism on the reversal of oxygen bubble formation was explained by Graves et al. as a high internal pO_2 causing initial growth of O_2 bubbles within the SOEC time period of each cycle. Then, when polarization is stopped, the pressure is released and the grain boundaries are healed by sintering back together at the high operating temperature. Also, it was discussed that during SOFC operation, re-sintering can mitigate the degradation mechanism, involving the heat generated during exothermic fuel-cell mode segments enhancing interface sintering (8).

Recently, lanthanide nickelates (Ln =La, Nd,Pr) have received considerable interest as an alternative to traditional lanthanum strontium manganites (LSM), cobaltites (LSC), ferrites (LSF) or cobalt ferrites (LSCF) oxygen electrodes for SOFCs and also as oxygen separation membranes (9,10).The main drawback of these nickelate phases is their reactivity with the standard electrolytes: yttria stabilized zirconia(YSZ) and gadolinium doped ceria (CGO) (11). For example, we have recently reported the integration of $Pr_2NiO_{4+\delta}$ oxygen electrodes into Ni–YSZ supported mT-SOFC using Ni–YSZ as the fuel electrode, YSZ as the electrolyte and a CGO:PNO composite active interlayer (12). It was shown that in despite of $Pr_2NiO_{4+\delta}$ decomposition into $PrNiO_3$ and PrO_{2-y}, the deterioration in electrochemical performance of the cell was completely eliminated by the addition of the CGO:PNO interlayer. We have demonstrated that there is an in-situ formation of a mixed praseodymium, cerium and gadolinium oxide (PCGO) at the interface between the electrolyte and the oxygen electrode, playing a crucial role in the stability and performance of the cell. Additional results about the excellent performance and stability under current load and alternated SOFC and SOEC cycles will be discussed in this paper. Another strategy to avoid the undesired reactivity between nickelates and YSZ during sintering is the direct formation of the nickelate phase into YSZ scaffolds after infiltration of precursor salts. We have recently proved this method for the case of $Nd_2NiO_{4+\delta}$ (NNO), by infiltration of neodymium and nickel nitrates followed by controlled calcination at temperatures below 900 °C (10). By this procedure, the formation of insulating zirconate phases was avoided leading to high and stable fuel cell performances.

Experimental details

Cell fabrication

NiO–YSZ anode supported tubes were fabricated by Powder Extrusion Molding (PEM), as described in previous works (13, 14). Subsequently, YSZ electrolyte suspensions were prepared using TZ-8YS (Tosoh) powders in an isopropanol–ethanol azeotropic mixture, and using PVB (polyvinyl butyral) as the binder and Beycostat as the dispersant agent. These suspensions were deposited by dip-coating, then dried at RT and co-sintered at 1500 ºC for 2 hours. Finally, PNO–CGO (4:1 in wt%) composite barrier layer was also deposited by dip coating (one immersion, sintered at 1100 ºC for 2 h). PNO powders (Marion Technologies) were used to produce the cathode suspensions in ethanol media, using PVB as the binder and Beycostat as the dispersant agent. Subsequently, the suspensions were deposited by dip-coating, dried at RT and sintered at 1100 ºC for 2 hours. Final dimensions of the microtubular cells, as seen in figure 1, were: 60 mm in length, outer diameter of 3.4 mm, NiO–YSZ wall thickness of about 700 μm, ~20 μm YSZ electrolyte, ~5 μm barrier layer and ~45 μm PNO oxygen electrode.

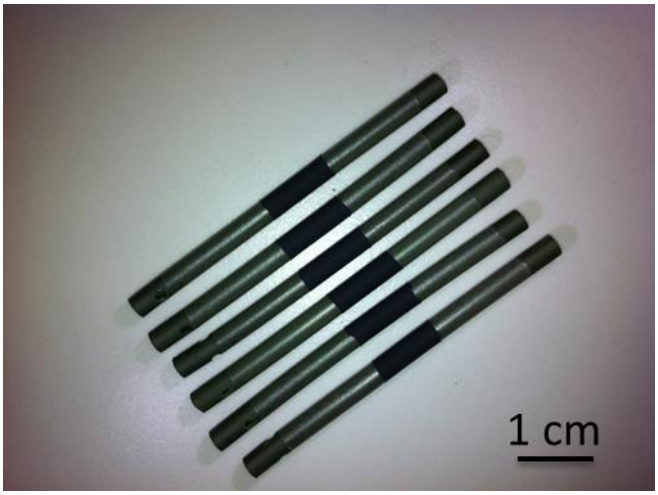

Figure 1. Typical microtubular cells fabricated at ICMA.

The infiltration of the $Nd_2NiO_{4+\delta}$ (NNO) phase was performed in collaboration with the group of Prof. Tom Etsell (Univeristy of Alberta). For this purpose, YSZ (previously calcined at 1500°C) was mixed and then applied to the sintered electrolyte by dip coating. The tube was then sintered at 1350°C. The subsequent infiltration of the Nd-nickelate was performed by using $Ni(NO_3)_2 \cdot 6H_2O$ and $Nd(NO_3)_3 \cdot 6H_2O$ mixtures, followed by calcination at temperatures between 800-1000 °C. Additional details can be found in reference (10).

In addition, symmetrical cells were fabricated in order to confirm the good behavior of PCGO as oxygen electrode for SOFC/SOEC applications. For this purpose, CGO powder (FuelCell Materials) was uniaxially pressed to form pellets. Three different compositions were tested as oxygen electrodes: pure PNO, PNO–CGO (4:1 in wt%) and PNO–CGO (1:4 in wt%), all of them deposited by screen-printing on both sides of the CGO pellets and sintered at 1100 ºC. Finally, dense PNO, PNO–CGO (4:1 in wt%) and PNO–CGO (1:4 in wt%) samples were also fabricated in order to perform oxygen diffusion studies. The density of all studied samples was >97%, as measured by the Archimedes method.

Electrochemical characterization

Electrochemical studies were performed at 600–800 ºC in both fuel cell and electrolysis modes using the experimental setup described in reference (15). A fuel composition of 50% H_2O –50% H_2 was used for operation in both fuel cell and electrolysis modes. The cells were sealed to alumina tubes using a ceramic sealant (Aremco, Ceramabond 503). Steam was supplied by the use of a direct vapour humidifier. All gas lines were externally heated in order to prevent steam condensation. Electrochemical experiments were performed using a VSP potentiostat/galvanostat (Princeton Applied Research, Oak Ridge, US). *j*–V (current density–voltage) was recorded in the galvanodynamic mode using a scan rate of 2.5 mA cm^{-2} s^{-1}.

EIS (electrochemical impedance spectroscopy) measurements were performed in complete microtubular cells, as well as in the symmetrical cells, using 20 mV of sinusoidal amplitude and a frequency range from 100 kHz to100 mHz using a VSP potentiostat/galvanostat (Princeton Applied Research, Oak Ridge, US) and a Zahner Zennium workstation (ZAHNER-elektrik GmbH &Co. KG, Germany).

ECR (electrical conductivity relaxation) measurements were performed in dense bar samples (18x5x2 mm^3) using a Probostat (NorEcs, Norway) test rig. Samples were annealed at 800 ºC and leaved under stabilization under different pO_2 ranging from 0.1 to 1 atm.

Microstructural characterization

SEM analysis was carried out on polished transverse cross-section samples using a Merlin field emission SEM (Carl Zeiss, Germany).

Results and discussion

Development of nickelates by infiltration

The first approach in order to integrate nickelate phases into the oxygen electrode of a SOC is the direct formation of the nickelate phase into YSZ scaffolds by infiltration. This was achieved after calcination at temperatures of about 1000 ºC (10). Although some NiO and Nd_2O_3 still remain unreacted, it does not affect the electrical performance of the cell, as these oxides exhibit reasonable electrical conductivity at the cell operating temperatures. Using infiltration techniques, different microtubular cells of Ni-YSZ/YSZ/NNO-YSZ were fabricated. The microstructure of the YSZ/NNO-YSZ interface and a detailed image of the NNO-YSZ oxygen electrode after operation is shown in figure 2. As observed, there is a connected network of NNO-based nanoparticles ranging from 50 to 100 nm.

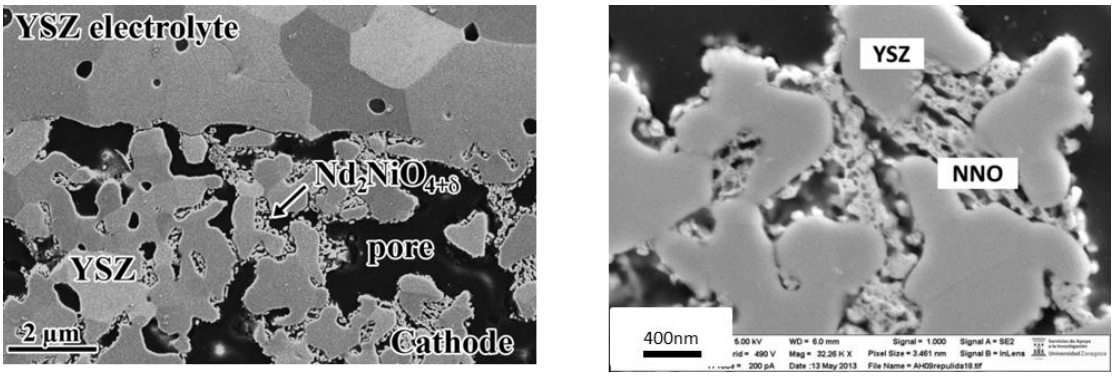

Figure 2. Typical microstructure of a NNO-YSZ oxygen electrode in the microtubular cell; (left) detail of the interface with the electrolyte and (right) detail of the NNO nanoparticles infiltrated into the YSZ matrix.

Remarkable performances were recorded for these cells. For example, at 800 ºC, power densities of about 0.76 Wcm^{-2} were achieved even at high voltages (0.8 V). In addition, no degradation was observed for up to 24 hours under current load at 600ºC, although longer durability studies are needed in order to confirm the good stability of the nanoparticles.

Development of active barrier layers for nickelate integration

As explained in the introduction section, another strategy to avoid reactivity is the development of barrier layers. For the $Pr_2NiO_{4+\delta}$ (PNO), we have recently reported that the use of a CGO interlayer produces an in-situ reaction between PNO and CGO, forming mixed praseodymium, cerium and gadolinium oxide (PCGO) at the electrolyte-oxygen electrode interface (12). The formation of this new phase plays a key role for the good stability and performance of the cells. In fact, current densities of about 600 $mAcm^{-2}$ at 0.7 V and 800 °C, and about 980 $mAcm^{-2}$ at 1.2 V and 800 °C were achieved in SOFC and SOEC modes, respectively. A summary of the electrochemical properties is summarized in figure 3. In addition, we have recently reported that combining SOFC and SOEC cycles, some of the decay in terms of current density during SOEC mode could be recovered (16), as also shown by other authors (7, 17). In any case, further research is needed to find the limits under continuous SOEC operation in order to avoid irreversible damage.

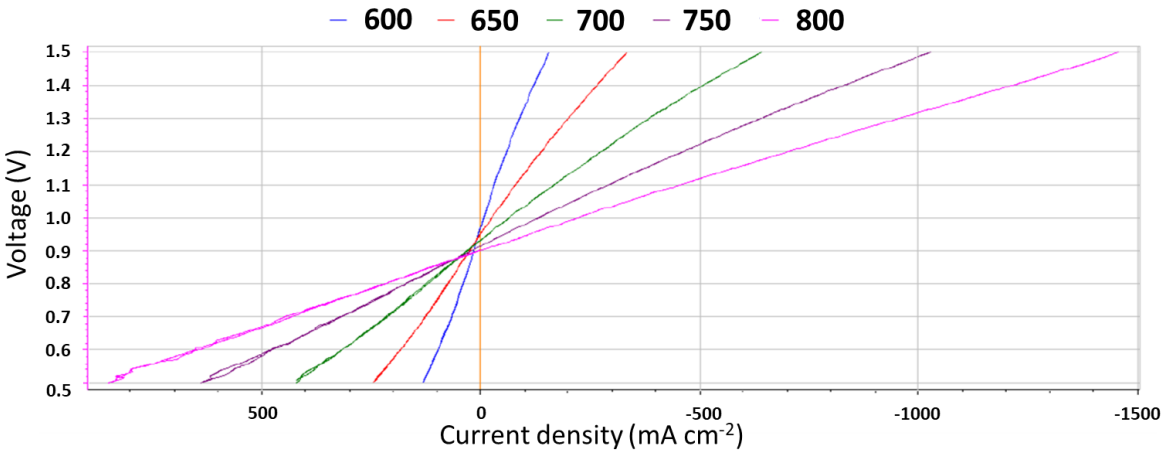

Figure 3. *j*-V curves in SOFC/SOEC modes collected at temperatures between 600 ºC and 800 ºC, using a gas composition of 50% H_2O – 50% H_2 at the fuel electrode and static air at the oxygen electrode.

Electrical studies of the PCGO phase

In order to confirm the good behavior of PCGO as oxygen electrode for SOFC/SOEC applications, symmetrical cells using CGO as the electrolyte and three different compositions as oxygen electrodes (PNO, 80PCGO and 20PCGO) were fabricated. Electrochemical impedance spectroscopy (EIS) measurements were performed, as shown in figure 4. The experiments were performed at temperatures between 850 ºC and 700 ºC

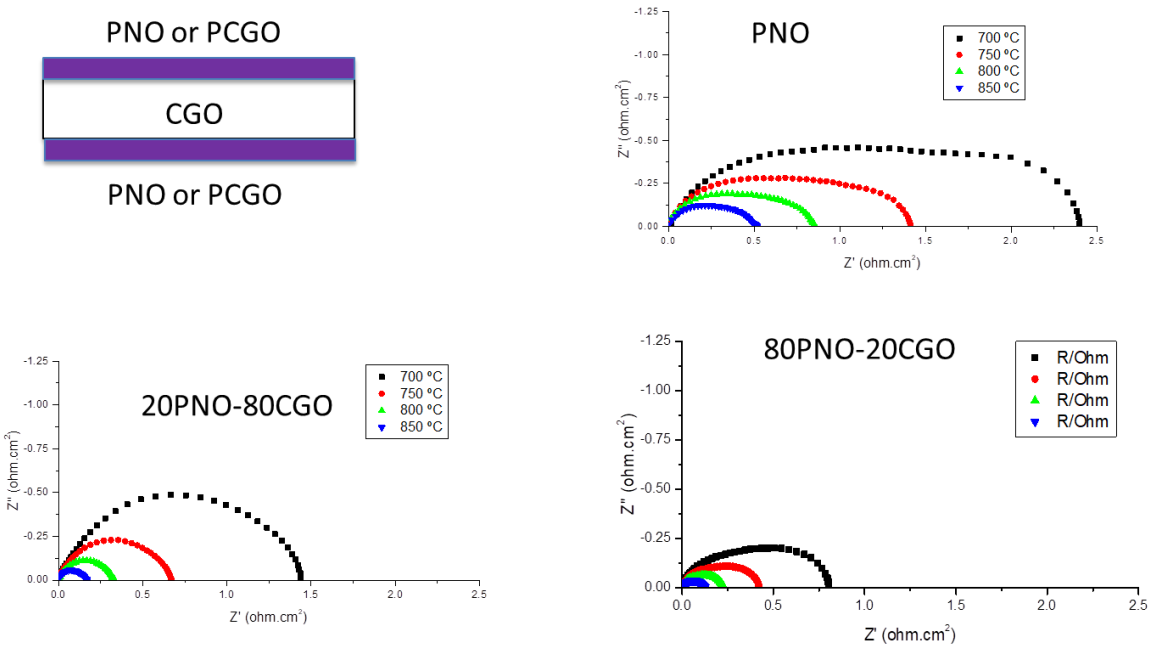

Figure 4. Symmetrical cell EIS experiments collected under OCV at 800 ºC for the PNO, 80PCGO and 20PCGO samples.

This experiment confirmed that both 80PCGO and 20PCGO presents lower ASR than pure PNO. For example at 700 ºC, ASR for the PNO sample is 2.4 Ωcm^2, whereas this value is significantly reduced to 1.45 Ωcm^2 and 0.78 Ωcm^2 for the 20PCGO and 80PCGO samples, respectively. In addition to possible microstructural differences, the effect of the in situ formed PCGO phase could help to a better adhesion to the CGO electrolyte and also could avoid reactivity of the PNO with the YSZ electrolyte. Additional DRT (distribution of relaxation times) analysis from EIS measurements and also microstructural studies are currently being conducted in order to fully understand the obtained results.

Finally, electrical conductivity relaxation (ECR) experiments were performed at 800 ºC for the PNO, 80PCGO and 20PCGO samples, in order to study their diffusion properties. An example of the ECR analysis is shown in figure 5, and a summary of the *D* (oxygen diffusion) and *k (*surface exchange coefficient) values is shown in table I. ECR fitting was performed following the procedures described by Ciucci (18,19).

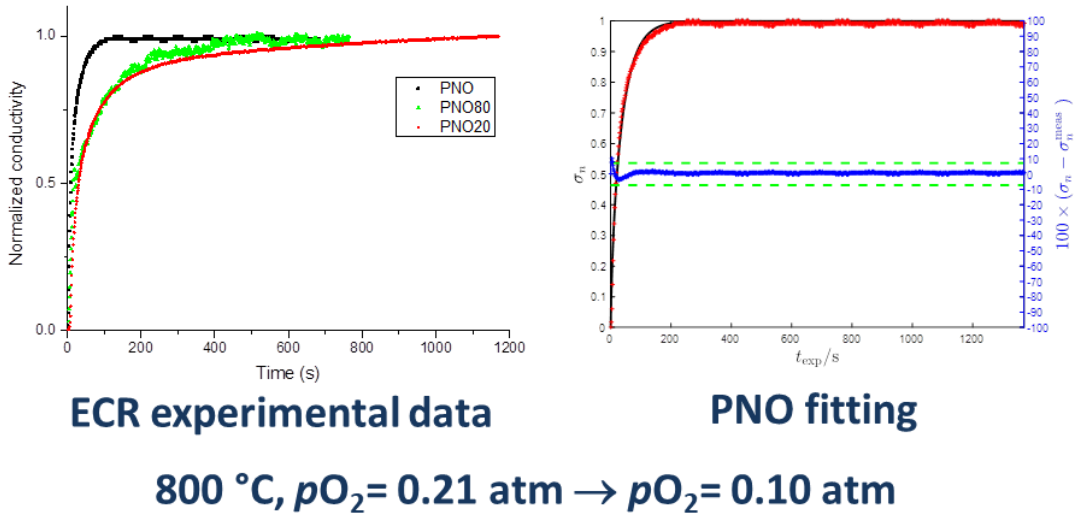

Figure 5. Electrical conductivity relaxation (ECR) experiments collected under at 800 ºC for the PNO, 80PCGO and 20PCGO samples (left); example of fitting for the PNO sample (right).

TABLE I. Summary of the different D_{chem} and k_{chem} values for the studied materials

Sample	D_{chem} (cm^2s^{-1})	k_{chem} (cm^2s^{-1})
PNO	3.24×10^{-8}	6.69×10^{-6}
80PCGO	1.06×10^{-8}	3.81×10^{-6}
20PCGO	1.47×10^{-8}	3.82×10^{-6}

These results showed that the PNO sample presents the highest *D* values, although both 80PCGO and 20PCGO samples present reasonable values to be used as an oxygen electrode for SOC applications. Those findings support the hypothesis that the in situ formed PCGO phase is helping the adhesion at the electrode/electrolyte and also could avoid YSZ/PNO reactivity, as shown by EIS analysis of the symmetrical cells.

Conclusions

We have presented to alternatives in order to integrate nickelate phases as oxygen electrodes into high efficient and durable SOCs. Both the impregnation route and the integration of active barrier layers need further development. In addition, we have shown that the new PCGO phase could be also used as an interesting alternative to the traditional oxygen electrode materials.

Acknowledgments

This work was funded by the MAT2015-68078-R project, financed by the Spanish Government (Ministerio de Economía y Competitividad) and the Feder Program of the

European Union. Prof. Etsell and Dr. Hanifi from University of Alberta are also acknowledged for NNO infiltration. The use of Servicio General de Apoyo a la Investigacion-SAI, Universidad de Zaragoza is finally acknowledged for the use of the electron microscopy facilities.

References

1. M. A. Laguna-Bercero, *J. Power Sourc.*, **203**, 4 (2012).
2. A. V. Virkar, *Int. J. Hydrogen Energy*, **35**, 9527 (2010).
3. H. T. Lim, A. V. Virkar, *J. Power Sourc.*, **180**, 92 (2008).
4. J. Schefold, A. Brisse, M. J. Zahid, *J. Electrochem. Soc.*, **156**, B897 (2009).
5. M. A. Laguna-Bercero, R. Campana, A. Larrea, J. A. Kilner, V. M. Orera, *Fuel Cells*, **11**, 116 (2010).
6. J. R. Mawdsley, J. D. Carter, A. J. Kropf, B. Yildiz, V. A. Maroni, *Int. J. Hydrogen Energy*, ***34***, 4198 (2009).
7. C. Graves, S. D. Ebbesen, S. H. Jensen, S. B. Simonsen, M. B. Mogensen, *Nature Mater.*, **14**, 239 (2015).
8. A. Hauch, K. Brodersen, M. Chen, M. B. Mogensen, *Solid State Ion.*, **293**, 27 (2016).
9. S. J. Skinner and J. A. Kilner, *Solid State Ion.*, **135,** 709 (2000).
10. M. A. Laguna-Bercero, A. R. Hanifi, H. Monzón, J. Cunningham, T. H. Etsell and P. Sarkar, *J. Mater. Chem. A*, **2**, 9764 (2014).
11. A. Montenegro-Hernandez, J. Vega-Castillo, L. Mogni, A. Caneiro, *Int. J. Hydrogen Energy*, **36**, 15704 (2011).
12. .M. A. Laguna-Bercero, H. Monzón, A. Larrea, V. M. Orera, *J. Mater. Chem. A*, **4**, 1446 (2016).
13. B. I. Arias-Serrano, M. E. Sotomayor, A. Várez, B. Levenfeld, H. Monzón, M. A. Laguna-Bercero, A. Larrea, *RSC Adv.*, **6**, 19007 (2016).
14. H. Monzón, M. A. Laguna-Bercero, A. Larrea, B. I. Arias, A. Várez, B. Levenfeld, *Int. J. Hydrogen Energy*, **39**, 5470 (2014).
15. M. A. Laguna-Bercero, A. Ferriz, A. Larrea, L. Correas, V. M. Orera, *Fuel Cells*, **13,** 1116 (2013).
16. M. A. Morales-Zapata, A. Larrea, M. A. Laguna-Bercero, *Int. J. Hydrogen Energy*, in press (2019).
17. J. Myung, D. Neagu, D. N. Miller, J. T. S. Irvine, *Nature*, **537**, 528 (2016).
18. F. Ciucci, *Electrochim Acta*, **87,** 532 (2013).
19. F. Ciucci, *Solid State Ion.*, **232**, 97 (2013).